The influence of deposition temperature and material stress on low-loss silicon nitride films for integrated quantum optics

Tareki, Abubaker M.; Kupchak, Connor; Mnaymneh, Khaled

Publisher's version / Version de l'éditeur:
https://doi.org/10.1109/JPHOT.2023.3284204
IEEE Photonics Journal, 15, 4, pp. 1-7, 2023-06-08

The Influence of Deposition Temperature and Material Stress on Low-Loss Silicon Nitride Films for Integrated Quantum Optics

Abubaker M. Tareki, *Member, IEEE*, Connor Kupchak, and Khaled Mnaymneh

***Abstract*—We report on an optimization procedure for depositing low-loss silicon nitride films at temperatures of 760 °C and 820 °C using low-pressure chemical vapor deposition. They were characterized in terms of quality and compositional proximity to stoichiometric silicon nitride. Films deposited at 760 °C showed a higher stoichiometry, with a silicon-to-nitrogen ratio of 0.744, when compared to the 820 °C film, which had a ratio of 0.77. We found the film deposited at the lower temperature had a smoother surface and exhibited lower optical losses. We investigated the impact of film stress on the refractive index of the film and found that removing the backside nitride from the wafer after deposition has a major effect on refractive index values. When using these films for integrated nonlinear and quantum applications, such as frequency conversion or soliton generation, knowledge of how the index changes with wafer and fabrication processing is critical for predicting the correct geometries, and the concomitant group velocities, needed to realize such quantum technologies.**

***Index Terms*—Film deposition, film stress, microfabrication, nanotechnology, nonlinear refractive index, silicon nitride.**

I. Introduction

SILICON nitride has recently gained a lot of interest within the photonic device community as an attractive materials platform of choice for a wide range of applications including sensing, metrology, nonlinear optics, quantum information processing and telecommunications. Silicon and nitrogen are the two major elements of silicon nitride. Oxygen, hydrogen, and carbon are common impurities that affect the quality of silicon nitride films. Ideal silicon nitride films should have a stoichiometric composition where the silicon-to-nitrogen (Si/N) ratio is 0.75 and should be stable under high temperature and harsh chemical processing conditions. The refractive index of the stoichiometric silicon nitride films is slightly less than 2 and is a good indicator of stoichiometry, as a value greater than 2 implies a higher silicon content, which leads to higher optical losses. The material exhibits a diverse and versatile set of optical properties that span an extremely wide transparency band (e.g., UV to mid-IR) [1], [2], [3]. Having a refractive index slightly larger than silica and an extremely low coupling loss (<0.3 dB/facet) makes nitride an ideal choice for integrated quantum optics [4] and can result in the removal of complexities in optical fiber. Control of the fabricated thickness of a silicon nitride waveguide layer allows for excellent dispersion engineering and more compact device footprints. The 5-eV bandgap energy of the material prevents two photon absorption effects and enables high-energy applications. This also helps to prevent or control unintended Raman or Brillouin scattering, which can cause deleterious effects on quantum noise measurements. The nonlinear index of silicon nitride is ten times higher than silica ($\sim 2.0\times10^{-19}$ m^2/W) and allows for lower power requirements in chip-based optical processing and four-wave mixing generation [5]. Furthermore, and the most cost-effective point, is that device fabrication techniques are CMOS compatible. Two common methods for depositing silicon are: low pressure chemical vapor deposition (LPCVD) and plasma enhanced chemical vapor deposition (PECVD) [6]. LPCVD-grown nitride has far superior film quality when compared to PECVD-grown films. High operating temperatures, between 750°C and 850°C, with low deposition pressures, between 0.2 Torr and 2 Torr, are the reasons why film quality is better; under these thermodynamic conditions, impurities and non-stoichiometry have a harder time incorporating within the film and is the reason they have ultra-low optical losses and high nonlinear indices. A main disadvantage of LPCVD systems is the use of toxic, explosive, or corrosive gaseous reactants. However, evolution of nanofabrication safety systems has greatly minimized such concerns [7]. Typical values of the refractive index in these films vary from 1.95 to 2.1. LPCVD process parameters can be optimized to achieve stoichiometric compositions but at a cost of having very large, greater than 1 GPa film stress, that leads to relaxation processes causing film crazing and cracks. Hence, understanding, tracking, and controlling film stress is critical when fabricating photonic devices. Film stress can be tuned and can vary from a few hundred MPa to GPa tensile, depending on the LPCVD deposition conditions such as gases flow ratios, temperature, and pressure.

In this paper, we have investigated processes for LPCVD deposition of silicon nitride films at different temperatures and studied how different stress-control methods impact film stress. Furthermore, we studied the impact this stress has on the material composition, surface roughness, and refractive index,

Manuscript received 2 June 2023; accepted 6 June 2023. Date of publication 8 June 2023; date of current version 16 June 2023. This work was supported by the National Research Council of Canada through High Throughput and Secure Networks Challenge Program. *(Corresponding author: Abubaker M. Tareki.)*

Abubaker M. Tareki and Connor Kupchak are with Carleton University, Ottawa, ON K1S 5B6, Canada (e-mail: abubakertareki@cunet.carleton.ca; connorkupchak@cunet.carleton.ca).

Khaled Mnaymneh is with the National Research Council Canada, Ottawa, ON K1A 0R6, Canada (e-mail: khaled.mnaymneh@nrc-cnrc.gc.ca).

Digital Object Identifier 10.1109/JPHOT.2023.3284204

TABLE I
DEPOSITION RECIPES

Run #	Temp. (°C)	Pressure (mTorr)	DCS:NH_3 ratio	DCS (sccm)	NH_3 (sccm)	Total gas flow (sccm)
1	820	300	1:10 (0.1)	5	50	55
2	820	300	1:3 (0.33)	17.5	52	69.5
3	820	300	1:1 (1)	15	15	30
4	820	300	3:1 (3.3)	45	15	60
5	760	300	1:10 (0.1)	5	50	55
6	760	300	1:3 (0.33)	17.5	52	69.5
7	760	300	1:1 (1)	15	15	30
8	760	300	3:1 (3.3)	45	15	60

which are all critical parameters in designing and fabricating next-generation photonic devices.

II. DEPOSITION

In this work, we employed LPCVD as it offers a higher quality film of nitride with lower loss over PECVD due to less impurities (i.e., hydrogen bonds). The gases used for the deposition process are dichlorosilane (SiH_2Cl_2), also known as DCS, and ammonia (NH_3). The ratio of DCS/NH_3 will determine the film properties, specifically whether the film is silicon-rich or stoichiometric. Stoichiometric nitride films (ratio <1) exhibit less loss than the silicon rich films (ratio >1) [4]. However, the stress is generally higher, which leads to film cracking for thicknesses greater than 300 nm. This can be detrimental for some applications in integrated quantum optics [7], which require thicknesses to be above 500 nm. As will be explained in the stress control section, stress must be controlled or eliminated in device fabrication. A design of experiment (DOE) of the deposition process is shown in Table I. The temperature and the pressure were fixed at 820 °C and 300 mTorr, respectively, while the DCS/NH_3 gases ratio were varied from 0.1 to 3. These values were chosen based on prior reports [5], [8]. The process was then repeated at 760 °C. Films with thicknesses of 200 nm and 500 nm were deposited on both bare silicon wafers and silicon wafers with a 5 μm thermal oxide isolation layer. Better refractive index fits can be achieved for depositions on bare silicon while the actual device fabrication will take place on wafers with thick oxide isolation layers. For film stress studies, the film thicknesses were 500 nm and 1000 nm, and both deposited on bare silicon and thick oxide isolation layers.

III. FILM CHARACTERIZATION

In this section, we describe the tools needed to gain information about the film properties.

A. Ellipsometry

The thicknesses and refractive index of the nitride films were measured using a variable angle spectroscopic ellipsometer (J.A.Woollam M2000). Ellipsometric spectra of the films were collected at three incident angles (50°, 60° and 70°) and over a wavelength range of 300 to 1700 nm. A Cauchy dispersion model was used to fit the film thickness and optical constants. Standard 2" silicon wafers were used in all experiments.

B. Chemical Wet-Etching Test

Tetramethylammonium hydroxide (TMAH) is common for etching silicon-rich films whilst stoichiometric nitride is used as a wet etch mask. A solution of 25% TMAH was used to investigate whether our films were stoichiometric or not. Thicknesses of the nitride samples were measured both before and after being immersed for 8 hours in the TMAH solution (@ 80°C).

C. SEM, XPS, FTIR and AFM

A scanning electron microscope (SEM) was used to take images of films for both deposition temperatures and to verify film thickness. The chemical composition of silicon nitride films was analyzed by X-ray photoelectron spectroscopy (XPS). The influence of the stress change between pre- and post-back-side-nitride-removal on the XPS measurement of same film at both temperatures was also investigated.

The main impurities are caused by the hydrogen bonding with the other elements in the film and are a source of optical propagation loss. The characteristics of hydrogenation and its band status in various silicon nitride films were analyzed by Fourier Transform Infrared Spectroscopy (FTIR). In general, there are four peaks at 843, 1184, 2183, and 3340 cm-1 in the spectra, which correspond to the Si-N stretching, N-H bending, Si-H stretching, and N-H stretching vibration modes, respectively [8], [9]. FTIR measurements were performed on the films before and after the backside nitride was etched to compare the effect of the stress on vibration modes.

Atomic Force Microscope (AFM) was also performed on films to evaluate the surface roughness, which is a metric of the film quality and grain packing. AFM measurements were done for pre- and post-backside silicon nitride etching.

D. Film Loss Measurement (Metricon)

The Metricon Model 2010/M was used to evaluate the film loss. It utilizes a surface-mounted prism coupling technique to measure both the thickness and refractive index. Specifically, a prism was pushed against the wafer surface to couple the light through the film at the desired wavelength as shown in Fig. 1. The decaying of the coupled light during its propagation across the wafer provides an estimate of the bulk material loss. The 2010/M's loss measurement option works over the range from 15 dB/cm to $\approx$ 0.1 dB/cm. Loss measurement near the lower limit of the tool may require further analysis with alternate methods to obtain the true values. Two nitride samples with a thickness of $\sim$ 380 nm (deposited at 760 °C and 820 °C respectively) were measured at 632.8, 983, 1312, and 1550 nm wavelengths.

IV. FILMS STRESS MEASUREMENTS AND STRESS CONTROL

A. Stress Measurements

A film stress measurement (FSM 900TC) tool was used to quantify the film stress at room temperature. This measurement

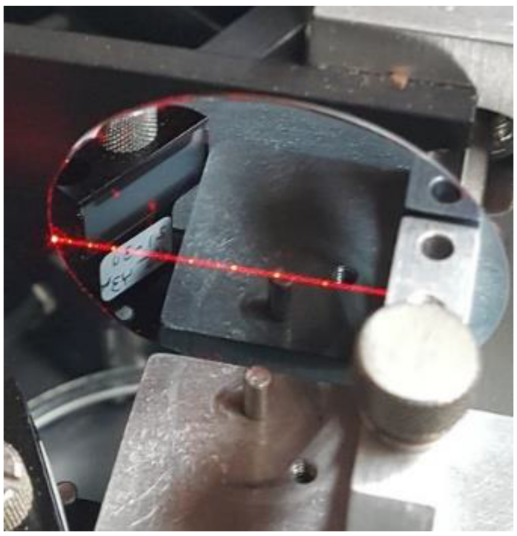

Fig. 1. Metricon measurement setup and the coupling light at 632 nm wavelength is propagating across the wafer which is used to estimate the bulk material loss (the white shining spots are scattered light due to particles in the light path).

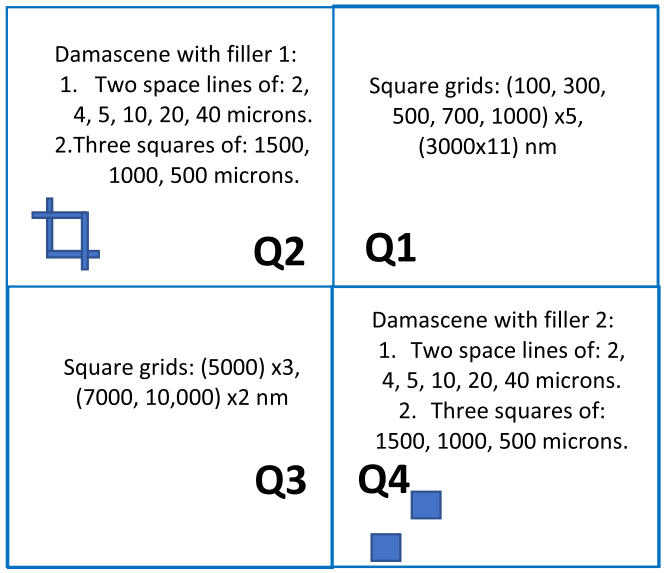

Fig. 2. Stress control mask layout of the four quadrants (2 × 2 inches each). The quadrants Q_1 and Q_3 consist of square grids varying from 100 nm to 10 mm. The quadrants Q2 and Q4 have two different damascene designs that have been used to control the stress and stop the crack in the deposited thick nitride films. Details of the mask designs are explained in the stress control section.

allows one to obtain the wafer bow height and can measure wafer's ranging from 2 to 8-inch. The stress values were evaluated based on the wafer bow pre- and post-nitride-backside-removal scan). Backside nitride removal was achieved by reactive ion etching (Vision 320 RIE). The process parameters used for removing the backside nitride films were 20 sccm CF4, 2 sccm O2, RF power of 100 W, and a process pressure of 300 mTorr.

B. Stress Control

The most convenient and fastest way to prevent cracks from propagating in the film was to use a diamond tip to scribe lines vertically and horizontally (shown in Fig. 3(a) and (b)) to section off crack free areas during device fabrication [7]. We patterned the oxide layer by using a photomask design (4 × 4 inches) as shown in Fig. 2 with 4 quarters (2 × 2 inches each). The quadrants Q_1 and Q_3 consist of square grids: 100, 300, 500, 700, 1000 of 5 rows each, 3000 of 10 rows in Q1 and 5000 of 3 rows, 7000, and 10000 of two rows each) in Q3. This photomask design will stop cracks from propagating and leave sufficient crack-free areas for device fabrication as shown in Fig. 3(c) and (d) [10]. Two stress-release damascene designs were used in Q_2 and Q_4. Q_2 forms an array of 10 × 10 of unit cells of dimension 5 mm × 5 mm with spacing of 1.5 mm used to put alignment marks for lithography processes. The Q_2 unit cell is composed of slabs of filler design with two spacings in-between filler slabs of 2, 4, 5, 10, 20, and 40 microns to simulate different spacing widths which may be used for waveguides or other devices fabrication. On a top of these gradual spaced slabs are three empty squares of 500, 1000, 1500 μm^2 with fillers around that would simulate device sizes like ring resonators. The Q_2 filler consists of overlapped rectangles (Damascene #1 design), and each has a dimension of 2 × 20 microns as shown in Figs. 2, 3(e) and (f) [11].

Similarly, the quadrant Q_4 is formed by an array of 10 × 10-unit cells of 5 mm × 5 mm each with spacing of 1.5 mm used to put alignment marks for lithography processes. The Q_4 unit cell is made of slabs of filler design with two spacings of 2, 4, 5, 10, 20, and 40 microns. Above the gradual spaced slabs are three empty squares of 1000 and 2000 μm^2 with surrounding filler that could be used for device fabrication such as ring resonators. The Q_4 filler consists of a periodic array of ∼ 5μm-size squares, with unit cells of two squares positioned in the 45° direction (Damascene #2 design). Alternate rows (columns) are spaced edge-to-edge by ∼ 9 μm. Adjacent rows (columns) are shifted edge-to-edge by ∼ 7 μm. This provides a critical spacing of ∼ 2.8 μm between two square corners in a unit cell and is shown in Figs. 2, 3(g) and (h) [12]. We had two runs with DCS/NH_3 ratio of 1/3 (17.5 sccm/ 51.4 sccm) at 820 °C and pressure of 300 mTorr. The first run was for wafers T-01 to T-06 with deposition time of 105 minutes and a target nitride thickness of 500 nm. The second run on wafers T-07 to T-12, a deposition time of 210 minutes was used to target a nitride thickness of 1000 nm. Each of these wafers was pre-patterned on the oxide layer before depositing the nitride film. This stress measurement data can be found in Table II.

C. Refractive Indices Change Due to Stress Value Change

The effect of the stress value on the refractive index before and after etching of the back side of the wafer was investigated. Two sets of six wafers were used to deposit nitride using recipe parameters: T = 820 °C, P = 300 mTorr, DCS/NH_3 = 1/3 (17.5 sccm/ 51.4 sccm).

The first run targeting a 200 nm thickness (38 min of deposition step) to be deposited of 3 bare silicon wafers (2-in wafers

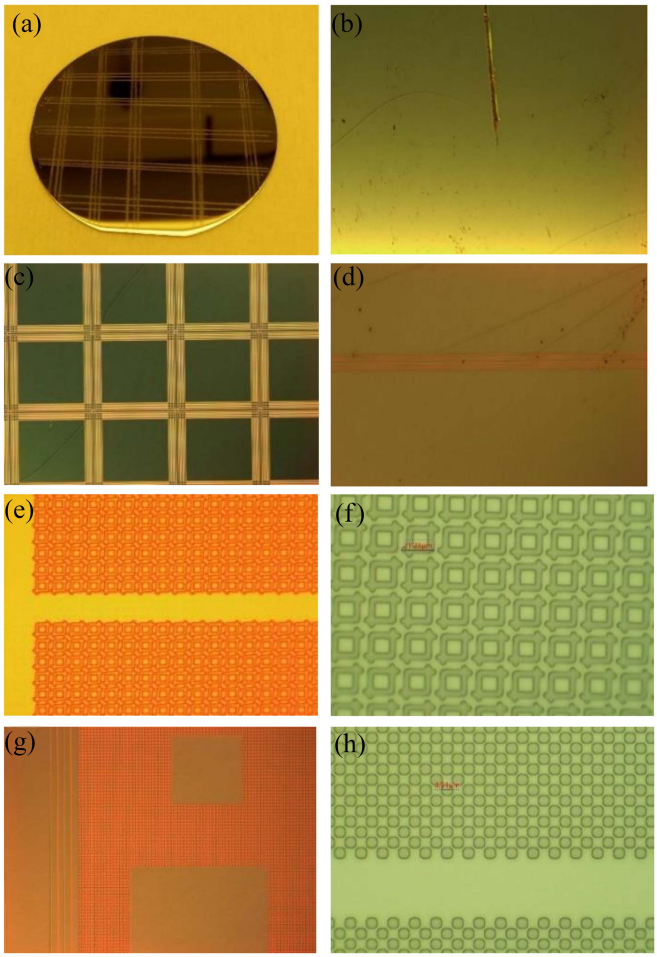

Fig. 3. Fabricated and patterned structures: (a) Full 2-inch wafer scribed with diamond pen within a grid formation to stop the cracks and leave sufficient area for device fabrication. (b) Cracks were stopped from propagating across the wafer by the scribed lines. (c) Pre-patterned squares of 500 μm^2 (Q_1 design) on the oxide before the nitride deposition and it shows how the cracks are prevented from propagating. (d) Pre-patterned large square of 5 mm $\times$ 5 mm (Q_3 design) used to prevent crack formation. (e) Q_2 Damascene design #1 is shown with no cracks in the 40 μm spacing between two filler 1 slabs. (f) Zoomed in view of the Q_2 filler 1 design. g) Q_4 Damascene design #2 is shown with no cracks inside two squares of sizes 1 mm^2 and 2 mm^2 with filler 2 design filling around these squares. (h) Closer look into Q_4 unit cell which shows that no cracks appear in the 40 μm spacing between two filler 2 slabs.

TABLE II
STRESS MEASUREMENTS

Wafer ID	Nitride thick. (nm)	Dep. Rate (nm/min)	Ref. Index (n)	Stress (MPa)	Oxide pre-Patterning description
T-01	586	5.58	1.986	1116	None
T-02	586	5.58	1.972	1076	diamond scribing
T-03	586	5.58	1.983	538	Q_1 Squa. 0.1 – 3 mm
T-04	586	5.58	1.969	608	Q_2 Damas. #1 design
T-05	586	5.58	1.989	481	Q_3 Squa. 5, 7, 10 mm
T-06	586	5.58	1.978	620	Q_4 Damas. #2 design
T-07	1190	5.67	1.973	1118	None
T-08	1190	5.67	1.988	1018	diamond scribing
T-09	1190	5.67	1.969	493	Q_1 Squa. 0.1 – 3mm
T-10	1190	5.67	1.975	537	Q_2 Damas. #1 design
T-11	1190	5.67	1.972	484	Q_3 Squa. 5, 7, 10 mm
T-12	1190	5.67	1.959	600	Q_4 Damas. #2 design

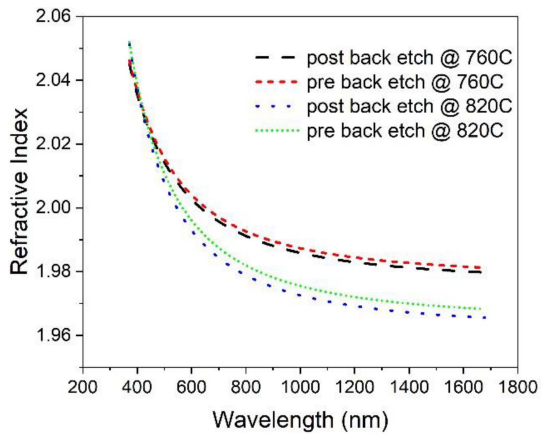

Fig. 4. Measured refractive index by ellipsometer for silicon nitride films of 500 nm thicknesses deposited at 760 °C and 820 °C, before and after the back side nitride removal. The graph shows a decrease in the refractive index value with the stress increase value after etching the back side nitride of the wafer.

Si-13, Si-14, and Si-15) and 3 oxide wafers (2-in wafers T-13, T-14, and T-15). The second run targeted a 500 nm thickness (92 min of deposition step) to be deposited on 3 bare silicon wafers (2-in wafers Si-16, Si-17, and Si-18) and 3 oxide wafers (2-in wafers T-16, T-17, and T-18).

V. RESULTS AND DISCUSSIONS

The recipe ratio of 0.3 DCS/NH_3 was found to be the optimum ratio for stoichiometric nitride films based upon the above characterization techniques. This recipe was used to deposit nitride films at the two temperatures of 760 °C and 820 °C while the pressure was kept at 300 mTorr.

The deposition rates and refractive indices for films deposited at 760 °C and 820 °C were 2.49 nm/min and 1.985 (1.36 mean squared error (MSE)), and 5.5 nm/min and 1.9723 (1.48 MSE), respectively. The measurement wavelength was 1550 nm. Both values of the refractive indexes fall well within the range of stoichiometric silicon nitride ($\sim \leq 2.1$, which depends on the wavelength, as shown in Fig. 4). Note that for some wavelengths, the value of the refractive index for the 760 °C film is lower than the 820 °C film. The deposition rate at 760 °C is lower than the value at 820 °C ($< 50\%$). The lower deposition rate leads to smaller grains and good compacting resulting in higher film quality and lower optical losses [5]. For both samples, the refractive index dependency on the wavelengths shows that it decreases as wavelength increases. Furthermore, it shows that for each film, the refractive index decreases when the stress increases after etching the backside nitride of the wafer. This

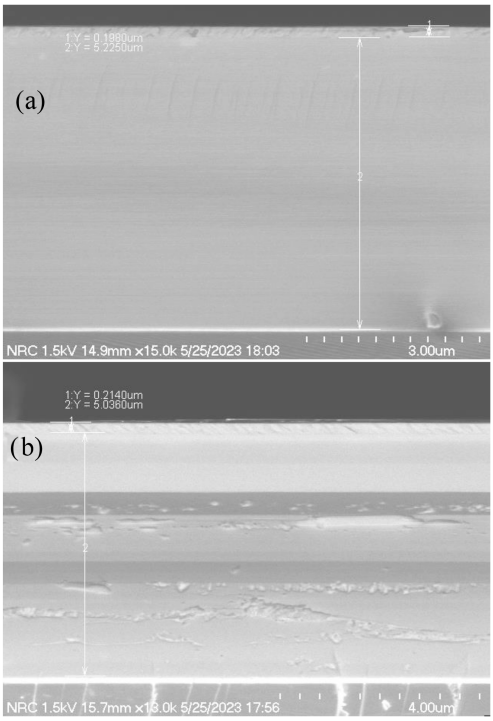

Fig. 5. SEM results show the nitride films deposited on the top of 5 μm of thermal oxide: (a) The stoichiometric silicon nitride film deposited at 760 °C has thickness of 198 nm. (b) The film deposited at 820 °C has thickness of 214 nm.

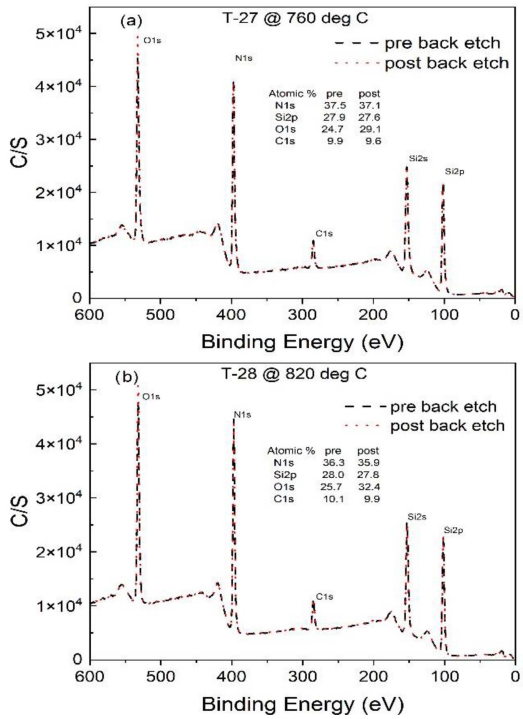

Fig. 6. XPS results show that: (a) The stoichiometric silicon nitride film deposited at 760 °C 0.744 and 0.743 ratio of Si/N before and after the back nitride removal, respectively. (b) The film deposited at 820 °C has 0.771 and 0.774 ratio of Si/N for the two cases, respectively.

phenomenon will be studied more and verified using multiple wafers with different substrates later in this section.

Another method to verify whether the nitride film is stoichiometric, or silicon-rich, is to use a TMAH solution. The thickness of our film was measured before and after the samples were immersed in at 80 °C for 8 hours. The thickness was found to be the same before and after the TMAH etching process and indicates the silicon nitride is stoichiometric.

Fig. 5(a) and (b) show cross-sectional SEM images for both films deposited at 760 °C and 820 °C, and the buried oxide isolation layer. The measured thickness of the films verifies what was measured using ellipsometry, which was around 200 nm. The XPS results in Fig. 6(a) and (b) show stoichiometric silicon nitride composition components. These components are evaluated in the atomic percentage of their presence found on the surface of nitride film, as shown in the graph. The ideal Si_3N_4 film has a ratio of Si/N components to be 3/4 (0.75). For the film deposited at 760 °C (T-27) the ratio found was $(27.9/37.5) = 0.744$, which is very close to being ideal, and $(27.6/37.1) = 0.743$ after backside nitride removal. This slight shift in the ratio might be due to the treatment of the surface during backside removal or tool error tolerance. The face of the wafer was covered with photoresist to protect it while etch and then the resist was stripped using O_2 plasma which explains the increase of the O_2 atoms presence in the film from 24.7 to 29.1%. On the other hand, the film deposited at 820 °C (T-28) was less stoichiometric, with a ratio of $28.0/36.3 = 0.771$ and post-backside removal of $27.8/35.9 = 0.774$. The presence of O_2 also increased from 25.7% to 32.4%. The change in the Si/N atoms ratio was not consistent in both cases, which may indicate that the shift is due to the tool tolerance and not a real change in the film composition. On the contrary, the O_2 presence increased in both films which supports the assumption of the O_2 plasma effect on the films. It seems deposition at the lower temperature yields better stoichiometry. This makes sense, as the lower the temperature becomes, the slower the deposition rate. This allows the chemical reaction between the gases to happen more fully resulting in less impurities in the newly deposited film and allows the formed grains to pack closely yielding smoother surfaces and expected lower optical losses.

FTIR analysis results are shown in Fig. 7(a) and (b). They illustrate that the absorption of the hydrogen in the nitride film is almost zero for films deposited at both 760 °C and 820 °C, before and after backside nitride removal. This proves that the stress increase on the wafer has no effect on the FTIR measurements. A strong peak is observed at 843 cm^{-1}(Si-N stretching) in all cases with no recorded peaks at 1184 cm^{-1} (N-H bending), 2183 cm^{-1} (Si-H stretching) and 3340 cm^{-1} (N-H stretching) for both LPCVD processes and indicates a dominant Si-N band in the film.

The AFM scan results shown in Fig. 8 of the 760 °C nitride film before and after backside nitride removal show a roughness average of 3.34 A° and 2.02 A°, and for the 820 °C film, are 3.56 A° and 2.38 A°, respectively. These values of roughness are indicative of the film quality and grain packing. This smoothness is on the order of a few angstroms and was measured directly after deposition, with no chemical mechanical polishing (CMP) or any other polishing technique. These results

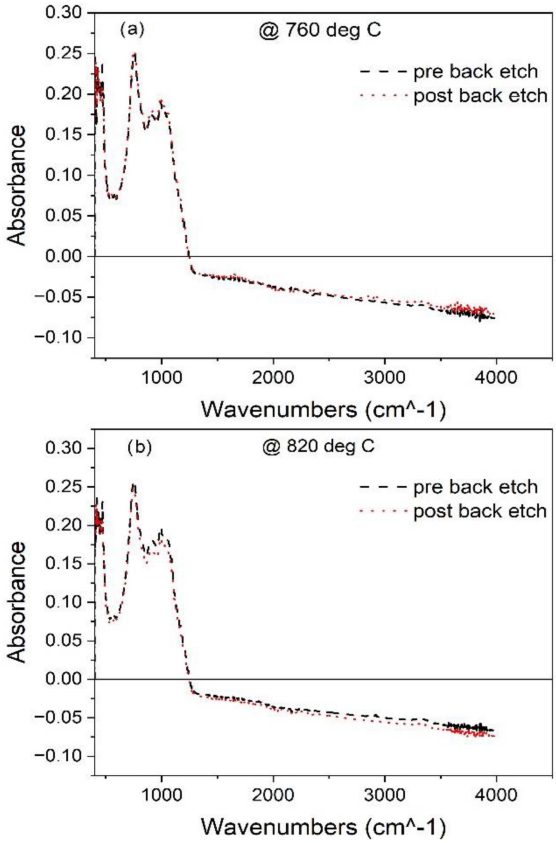

Fig. 7. FTIR results are almost identical for both cases before and after back side etch. (a) The stoichiometric silicon nitride film deposited at 760 °C with a strong peak at 843 cm−1 (Si-N stretching) and no other peaks. (b) The nitride film deposited at 820 °C exhibits a similar peak structure to the film deposited at 760 °C.

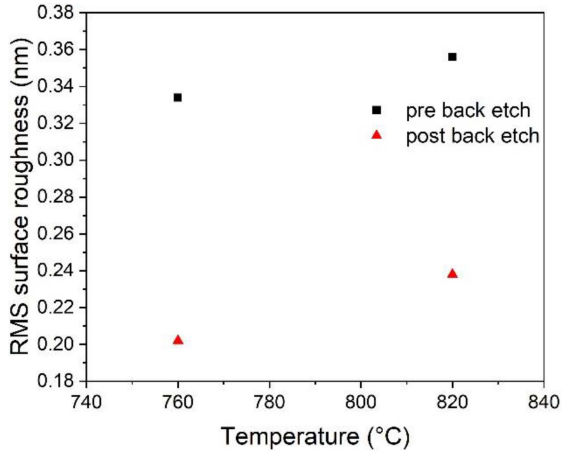

Fig. 8. AFM results show that the roughness decreases by 30% when the stress increases due to the removal of the back side nitride. The stoichiometric silicon nitride film deposited at 760 °C has average change of the roughness from 3.34 A° to 2.02 A°. The nitride film deposited at 820 °C has average change of the roughness from 3.56 A° and 2.38 A°.

are very promising because extremely smooth surfaces are important when it comes to integrating superconducting nanowires for single-photon detection. Nanometer roughness can lead to current-bunching giving false counts. The graph shows that the roughness values at both temperatures decreases by 30% when the stress increases due to etching the nitride film on the backside of wafer. This stress is tensile which means that the wafer will bow downward from its center (concave-curved inward). It is presumed that this bow will make the grains pack more which will result in smoother surface (less roughness) as measured.

The bulk nitride films (760 °C and 820 °C) were evaluated using a Merticon (2010M) at 632.8, 983, 1312, and 1550 nm wavelengths. At 760 °C, the Metricon yielded measurements of 0.21, 0.27, 0.51, and 1.09 dB/cm for the respective wavelengths. For silicon nitride deposited at 820 °C the losses were 0.17, 0.3, 0.32, and 1.1 dB/cm, respectively. For wavelengths of 632 nm and 983 nm, the losses are state-of-the-art. Values measured for 1312 nm and 1550 nm are more doubtful because the film thickness used was smaller than is needed for single-mode propagation at those wavelengths. Regardless, if these values represent unconfined modes, propagation losses of confined modes are expected to be beyond the ability of the Metricon tool to determine and other methods, such as the cutback method, will be needed to determine the true loss values. These loss values are close to the limitations of the device already and further investigation with other tools will be necessary to determine the true loss at all wavelengths of interest. The loss values at 1550 nm wavelength were difficult to measure (due to high sensitivity to existence of particles and cracks as the film is too stressful) for both samples and showed greater losses than the other wavelengths. This is contrary to what is typically expected as materials generally exhibit lower loss values at longer wavelengths.

Stress measurements in Table II show that the stress values for wafers T-01 to T-06 (500 nm) and for wafers T-07 to T-12 (1000 nm) were comparable $\sim$ 1116 MPa (in stoichiometric film range). The stress control methods used were effective in reducing the stress to the silicon-rich films in the range of 600 MPa or below, which typically does not exhibit cracks. The results show that scribing the wafer is a faster and easier way to reduce cracks, but it unfortunately fails to reduce the stress adequately enough to control the stress and eliminate cracking (1076 MPa for 500 nm thickness)**.** The pre-patterning designs of squares (Q_1 and Q_3) showed the lowest stress values ($\sim$ 500 MPa) and resulted in sufficient crack-free areas over a range of areas. Other pre-patterning damascene designs (Q_2 and Q_4) showed low stress values ($\sim$ 600 MPa) and crack-free areas favorable for fabricating devices. We believe that this surface stress reduction happens because of converting one large deposited slab of highly stressful stoichiometric nitride into smaller slabs using these pre-patterned structures. Etching the nitride on the back of the wafers caused a greater amount of stress and resulted in a change to the refractive index when measured before and after etching. Table III shows that in general, the refractive index decreased with increasing stress. The fourth column shows that the absolute difference of the stress values between pre and post wafer back etch was in the range of 700 – 1000 MPa for both silicon and oxide substrate wafers at both nitride thicknesses (200 and 500 nm). The last column displays the change in refractive indexes. In all cases, the index reduces in value slightly when the backside

TABLE III
STRESS VS REFRACTIVE INDEX (BEFORE AND AFTER WAFER NITRIDE BACK ETCH (BE))

Wafer ID	Stress Measurements (MPa)			Refractive index Measurements		
	pre-BE	post-BE	Stress Diff.	pre-BE	post-BE	Ref. index Diff.
Si-13	357	1098	741	1.969	1.9668	-0.0022
Si-14	208	990	782	1.9635	1.962	-0.0015
Si-15	381	1363	982	1.9642	1.9615	-0.0027
T-13	309	1190	881	1.9494	1.9481	-0.0013
T-14	300	1229	929	1.9492	1.9465	-0.0027
T-15	330	1205	875	1.9497	1.9465	-0.0032
Si-16	206	1147	941	1.9779	1.9764	-0.0015
Si-17	244	1207	963	1.9735	1.9718	-0.0017
Si-18	115	1277	1162	1.9744	1.9729	-0.0015
T-16	234	1270	1036	1.9628	1.9612	-0.0016
T-17	299	1304	1005	1.9609	1.9606	-0.0003
T-18	320	1274	954	1.9628	1.9546	-0.0082

nitride is removed. While these index changes seem small, they are enough to make group velocities at interband frequencies unequal ruining nonlinear conversion efficiencies [13].

VI. CONCLUSION

Deposition methods and their parameters are critical in determining the overall quality and characteristics of fabricated silicon nitride films. Generally, LPCVD (>700 °C) is a preferred deposition method over PECVD (~ 400 °C) as LPCVD leads to the production of higher quality films that contain less hydrogen bond impurities due to the higher temperatures. The ratio of NH_3 and DCS gases used in the LPCVD process ultimately affects the final Si/N ratio of the fabricated film. Each recipe (i.e., gas flow ratio) results in a specific deposition rate, grain-packing, refractive index, and residual stress. In this study, we investigated different DCS/NH_3 gas ratios and found an optimum ratio of 17.5 sccm/52 sccm $= 0.3$. Once identified, we performed further investigation into the quality of LPCVD deposited films at two different temperatures of 760 °C and 820 °C. Our results showed that films deposited at 760 °C exhibited a deposition rate (2.49 nm/min) that was 50% slower than those deposited at 820 °C (5.5 nm/min). Also, the results show that the refractive index values for both temperatures decrease with stress and increase after etching the nitride on the backside of the wafer. The stoichiometry of the films was evaluated using an 8-hour TMAH chemical etch at 80 °C. No etching was observed. Exact film composition was obtained through XPS and showed that the 720 °C film had a Si/N ratio of 0.744 while the film deposited at 820 °C was less stoichiometric with Si/N ratio of 0.771. The stress increase from backside nitride etching did not seem to have considerable impact on these ratios. The FTIR results showed peaks solely at 843 cm^{-1} for both films, before and after the backside etch, which indicated that only Si-N bonds were present. The AFM analysis illustrated that the average surface roughness of the films deposited at temperatures of 760 °C and 820 °C decreases by about 30% due to the stress increase (3.34 A° and 2.02 A°) and (3.56 A° and 2.38 A°), respectively. Different techniques, including some designs used for the damascene process, were evaluated for their ability to control and reduce stress. Lastly, we found that the refractive index of the film decreased with the increased stress due to etching the backside nitride. We found this increase of stress was consistent regardless of the substrate material under the nitride film (oxide or silicon) or the film thickness. In addition to having low-loss for single-photon operation, silicon nitride waveguides must have carefully controlled values of refractive index, as nonlinear optical processing of light depends upon second- and third-order dispersion and precise phase-matching conditions for integrated quantum optics. This work demonstrates that wafer and film processing may affect index values in a way that is unexpected resulting in unfavorable changes in the device performance, and so careful attention to fabrication steps are needed to ensure proper values of the refractive index are realized.

ACKNOWLEDGMENT

The authors gratefully acknowledge Robert Vandusen, Angela Mccormick, Rodney Aiton and Simona Moisa for their contributions to this work.

REFERENCES

[1] D. J. Blumenthal, R. Heideman, D. Geuzebroek, A. Leinse, and C. Roeloffzen, "Silicon nitride in silicon photonics," *Proc. IEEE*, vol. 106, no. 12, pp. 2209–2231, Dec. 2018.
[2] N. Hegedüs, K. Balázsi, and C. Balázsi, "Silicon nitride and hydrogenated silicon nitride thin films: A review of fabrication methods and applications," *Materials*, vol. 14, no. 19, Sep. 2021, Art. no. 5658.
[3] K. Jhansirani, R. S. Dubey, M. A. More, and S. Singh, "Deposition of silicon nitride films using chemical vapor deposition for photovoltaic applications," *Results Phys.*, vol. 6, pp. 1059–1063, 2016.
[4] R. Marchetti, C. Lacava, L. Carroll, K. Gradkowski, and P. Minzioni, "Coupling strategies for silicon photonics integrated chips," *Photon. Res.*, vol. 7, pp. 201–239, 2019.
[5] J. K. Author, "Optimisation and characterisation of LPCVD silicon nitride thin film growth," M.S. thesis, Dept. Microtech. and Nanosci., Chalmers Univ. Tech., Gothenburg, Sweden, 2006.
[6] H. El Dirani et al., "Ultralow-loss tightly confining Si_3N_4 waveguides and high-Q microresonators," *Opt. Exp.*, vol. 27, pp. 30726–30740, 2019.
[7] K. Luke, A. Dutt, C. B. Poitras, and M. Lipson, "Overcoming Si_3N_4 film stress limitations for high quality factor ring resonators," *Opt. Exp.*, vol. 21, pp. 22829–22833, 2013.
[8] C. Yang and J. Pham, "Characteristic study of silicon nitride films deposited by LPCVD and PECVD," *Silicon*, vol. 10, pp. 2561–2567, Nov. 2018.
[9] L. Vanzetti, M. Barozzi, D. Giubertoni, C. Kompocholis, A. Bagolini, and P. Bellutti, "Correlation between silicon-nitride film stress and composition: XPS and SIMS analyses," *Surf. Interface Anal.*, vol. 38, pp. 723–726, 2006.
[10] D. Li et al., "Characteristics of crack-free silicon nitride films deposited by LPCVD for photonic applications," *J. Electron. Mater.*, vol. 50, pp. 6862–6869, 2021.
[11] M. H. P. Pfeiffer et al., "Photonic damascene process for low-loss, high-confinement silicon nitride waveguides," *IEEE J. Sel. Topics Quantum Electron.*, vol. 24, no. 4, Jul./Aug. 2018, Art. no. 6101411.
[12] K. Wu and A. W. Poon, "Stress-released Si_3N_4 fabrication process for dispersion-engineered integrated silicon photonics," *Opt. Exp.*, vol. 28, pp. 17708–17722, 2020.
[13] Q. Li, M. Davanço, and K. Srinivasan, "Efficient and low-noise single-photon-level frequency conversion interfaces using silicon nanophotonics," *Nature Photon.*, vol. 10, pp. 406–414, 2016.